npj | precision oncology

Article

Published in partnership with The Hormel Institute, University of Minnesota

https://doi.org/10.1038/s41698-025-01146-7

Tumour-infiltrating leucocytes as prognostic biomarkers of bevacizumab-treated ovarian cancer patients results from the phase IV MITO16A/MaNGO OV-2 clinical trial

Eliana Pivetta[1,16,18], Vincenzo Canzonieri[2,3,18], Marina Bagnoli[4,18], Paolo Chiodini[5], Anna Spina[6], Laura Arenare[7], Domenica Lorusso[8,17], Giulia Tasca[9], Sabrina C. Cecere[10], Annamaria Ferrero[11], Giosuè Scognamiglio[12], Francesca Basso-Valentina[1], Daniela Califano[6], Loris De Cecco[4], Teresa Di Lauro[6], Milena S. Nicoloso[1], Martina Arcieri[13], Daniela Russo[6], Paola Spessotto[1], Stefano Indraccolo[14,15], Delia Mezzanzanica[4], Francesco Perrone[7], Sandro Pignata[10,19] & Gustavo Baldassarre[1,19] ✉

The treatment of Epithelial Ovarian cancer (EOC) could benefit from the addition of bevacizumab (BEV) to standard chemotherapy in selected patients. Gene expression (GE) profiling and the evaluation of immune infiltration are used to define patients' prognosis. However, their role as prognostic and/or predictive biomarkers for the efficacy of antiangiogenic therapy efficacy remains uncertain. In this study, we combined GE profiling and multiplex immunofluorescence (MIF) analyses on material from patients enrolled in the phase IV MITO16A/MaNGO OV-2 trial, assessing associations between immune infiltrate and patients' prognosis. Patients were stratified into four molecular subtypes, and CIBERSORTx was applied to infer the cell-type-specific expression pattern of immune populations. MIF evaluated the presence of immune cells in the tumor and stromal compartments. These complementary experimental approaches revealed that immune infiltration is associated with shorter progression-free survival in BEV-treated patients, warranting future investigation to evaluate its use as a viable biomarker for patient stratification. Trial registration: NCT01706120, EudraCT number: 2012-003043-29, Date of registration 24 September 2012.

In the last decade, two molecular targeting agents have been introduced for the treatment of Epithelial Ovarian Cancer (EOC): the anti-angiogenic agent bevacizumab (BEV) and the PARP inhibitors (PARPi). While the optimal application of PARPi is based on the molecular stratification of patients, this is still not established for BEV administration[1,2]. BEV is a humanized monoclonal antibody that, binding to vascular endothelial growth factor (VEGF), inhibits the activation of its receptor (VEGFR) and thus reduces tumor neoangiogenesis[3]. The combination of BEV with carboplatin and paclitaxel, followed by maintenance BEV, is a standard option in patients with newly diagnosed advanced EOC[1]. The addition of BEV to standard chemotherapy improved progression-free survival (PFS); however, the results were inconsistent in terms of overall survival (OS), and several studies have investigated, with limited results, the presence of markers of BEV efficacy[4–8].

Considering that a close relationship between inflammation and angiogenesis has emerged, considerable interest has been given to the role of inflammatory indices and the neutrophil–lymphocyte ratio (NLR), studied in peripheral blood, as predictors of BEV efficacy[9–11]. Recently, the MITO-24 study evaluated the role of these inflammatory indices in EOC and demonstrated that BEV improves clinical outcome in patients with a high

A full list of affiliations appears at the end of the paper. ✉e-mail: gbaldassarre@cro.it

NLR, but may be detrimental in those with a high systemic immune inflammation index[12,13]. However, to deeply analyze the impact of a possible involvement of immune components on anti-angiogenic treatments, particular attention should be given to the tumor microenvironment (TME), rich in several cell types (immune cells, fibroblasts, and adipocytes) and soluble factors interfering with tumor growth[14,15]. Indeed, it has been demonstrated that tumor inflammatory infiltrate could have both anti-tumor and pro-tumor roles[16]. Ovarian cancer TME is highly heterogeneous, displaying the presence of tumor-infiltrating lymphocytes (TILs), associated with increased survival, but also of immunosuppressive cells (e.g., T-Regs, Myeloid-suppressor cells, CAFs, etc.). Moreover, inter-patients variability has been constantly reported, which makes the characterization of this TME a complex issue (reviewed in refs. 16–18).

A standardized scoring system, originally studied in colorectal cancer, allows for the classification of tumors as "hot" or "cold", depending on the degree of infiltration of two lymphocyte subpopulations (CD3 and CD8), both in the center of the tumor and in the invasive margin. "Hot" cancers have high T cell infiltration, whereas "cold" tumors have little to no T cells or these are restricted to the periphery of the tumor[14]. $CD8^+$ T cells mediate specific cytotoxicity against tumor cells, causing direct lysis of cancer cells and the production of pro-inflammatory cytokines TNFα, IFNγ, and IL-2[15].

Currently, no clear data are available on the correlation between BEV response and TILs in EOC. The only small retrospective study we found suggested an association between lymphocyte infiltration and shorter PFS in patients treated with BEV respect to patients treated with chemotherapy alone[19]. Moreover, the analyses of EOC molecular subtypes in samples from patients included in the ICON7 clinical trial[6], indicated that the immune-related subtype, usually associated with better prognosis, might have a comparably smaller benefit[20] or a detrimental effect[21] from treatment that includes BEV.

These data could indicate that the presence of TILs might have a different prognostic significance in BEV-treated EOC patients. On the other hand, they require validation in independent cohorts of patients to eventually help identify patients who are less likely to benefit from BEV maintenance therapy.

We explored this possibility with the MITO16A-MaNGO OV-2 phase 4 trial, designed and conducted to assess the clinical and biological prognostic factors for advanced EOC patients receiving first-line treatment with carboplatin, paclitaxel, and BEV[22,23]. We combined gene expression profile (GEP) and, for the first time in a multicenter clinical trial in EOC, a multiplex immunofluorescence (MIF) approach that allowed us to precisely distinguish between immune cells infiltrating the tumors from those present in the stromal part and to define their prognostic impact in a large population of EOC patients homogeneously treated in first line with BEV.

Results

Molecular stratification indicates a poorer prognosis for immune-related subtypes treated with BEV

In the past years, many efforts have been made to characterize EOC molecular subtypes with prognostic impact based on their GEP. Starting from the Tothill study[24], different algorithms have been generated and, although some differences are evident, a general consensus has been developed around the existence of four major molecular subtypes, which can be recapitulated as immunoreactive (the one with better prognosis), differentiative, proliferative, and mesenchymal, the latter two having the worst prognosis. Based on this classification, a previous study on samples from patients enrolled in the ICON-7 trial suggested that the proliferative and mesenchymal molecular subtypes (the ones with the poorest survival) had a greater benefit from treatment that includes BEV. Yet, the median PFS of patients belonging to the four different subtypes treated with BEV was largely superimposable (proliferative, 21.9 months; differentiated, 21.6 months; immunoreactive, and mesenchymal, 20.8 months)[20]. These data suggested that the immunoreactive and differentiated subtypes were not biomarkers of good prognosis when BEV was added to the carbo-taxol treatment.

Table 1 | Clinical and pathological characteristics of patients with biomarker analysis

	Population enrolled (n = 398)		Patients in analysis for GE (n = 197)		Patients in analysis for MIF (n = 292)	
Median age (IQR)	59.1 (49.8–66.5)		59 (50–66)		59.1 (49.8–66.5)	
Age category	n	(%)	n	(%)	n	(%)
<65	278	(70)	140	(71.1)	202	(69.2)
≥65	120	(30)	57	(28.9)	90	(30.8)
ECOG performance status						
0	315	(79.2)	166	(84.3)	234	(80.1)
1	69	(17.3)	29	(14.7)	51	(17.5)
2	14	(3.5)	2	(1)	7	(2.4)
Residual disease						
None	153	(38.4)	91	(46.2)	115	(39.4)
≤1 cm	72	(18.1)	42	(21.3)	60	(20.5)
>1 cm	120	(30.2)	60	(30.5)	90	(30.8)
Not operated	53	(13.3)	4	(2)	27	(9.2)
FIGO stage						
IIIB	36	(9.1)	23	(11.7)	27	(9.2)
IIIC	275	(69.1)	138	(70)	207	(70.9)
IV	87	(21.9)	36	(18.3)	58	(19.9)
Tumor histology						
High-grade serous	333	(83.7)	173	(87.8)	254	(87.0)
Low-grade serous	13	(3.3)	7	(3.6)	9	(3.1)
Endometrioid	9	(2.3)	5	(2.5)	8	(2.7)
Clear cell	11	(2.8)	6	(3.1)	10	(3.4)
Mucinous	3	(0.8)	0	0	1	(0.3)
Mixed	4	(1.0)	2	(1)	2	(0.7)
Other	25	(6.3)	4	(2)	8	(2.7)

Here, we applied the algorithms developed in two major studies[24,25] to the GEP of the 197 EOC samples (173 of which were high-grade serous ovarian cancer (HGSOC)) from the MITO16A-MaNGO OV-2 trial (indicated as MITO16A in Figures) that passed all the quality controls (Fig. S1). No differences in clinical and pathological variables were observed between patients included in GEP analysis (n = 197) and the whole MITO16A-MaNGO OV-2 trial population (n = 398), except for a slight increase in patients with no residual disease (Table 1).

We observed that the two algorithms differentially allocated patients within the four different subtypes, in agreement with previous observations[26,27]. The same differential distribution was evident when applying the classifiers to all histologies or only to the HGSOC cases included in the MITO16A-MaNGO OV-2 study (Fig. S2).

Interestingly, the prognostic assessment according to the molecular subtypes classification of the HGSOC included in the MITO16A-MaNGO OV-2 cohort showed that, regardless of the classifier applied, the mesenchymal subtype (MES/C1) had a better prognosis than expected with a median progression free survival (PFS) of 37 months (95% CI: 29–NA) using the TCGA classifier (Fig. 1A) and of 29 months (95% CI: 24–42) using the Tothill classifier (Fig. 1B). Concurrently, the immune subtypes (IMM/C2) unexpectedly performed worse than the MES/C1 subtype, with a median PFS of 25 months applying both the TCGA (95% CI: 19–NA) and Tothill (95% CI: 18–NA) classifiers (Fig. 1A, B). These data suggested that the addition of BEV to standard chemotherapeutic treatment differently affects the prognosis of these two molecular subtypes, with a detrimental effect for the specific subgroup of patients characterized by a more pronounced immune-related transcriptomic profile, as suggested by others[20,21].

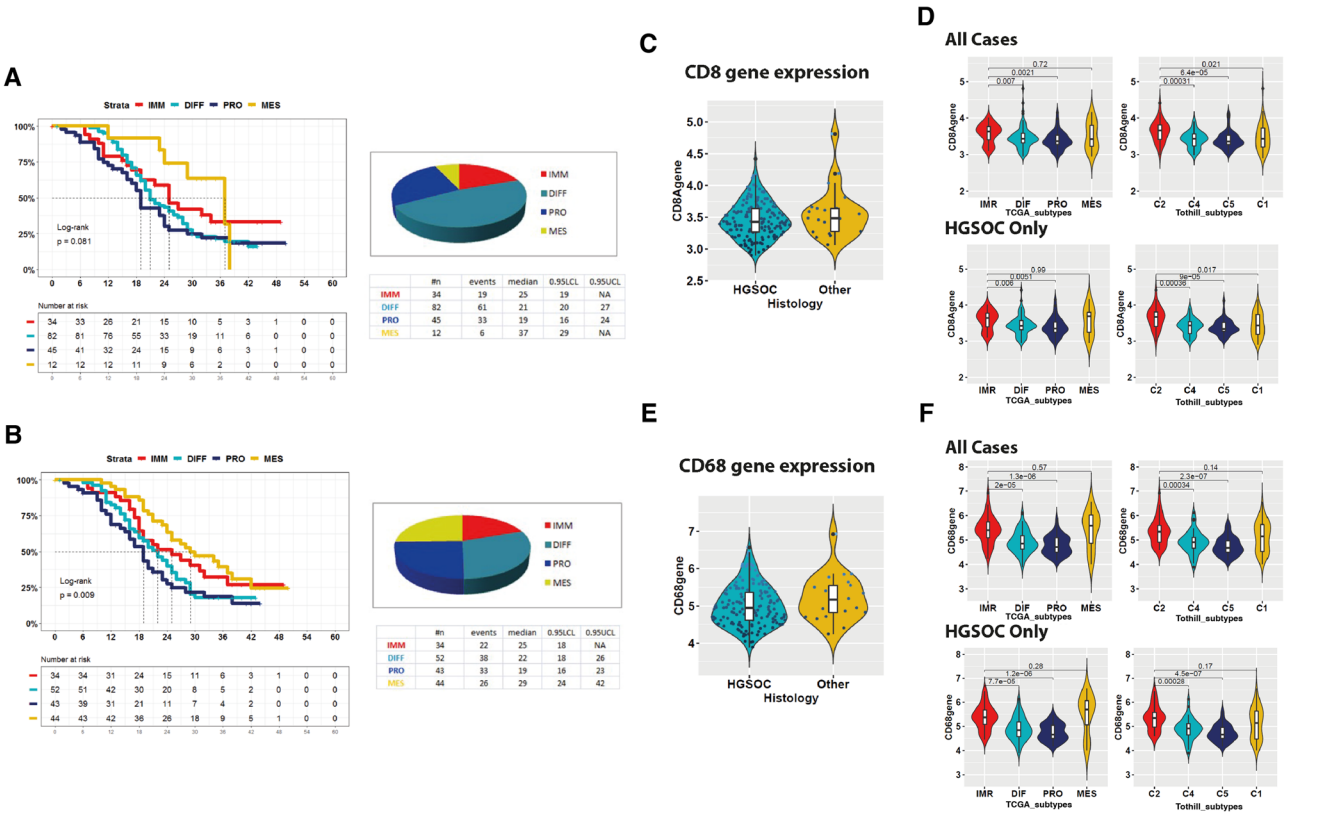

Fig. 1 | Molecular subtypes of samples from the MITO16A case material. Progression-free survival stratification risk according to TCGA (**A**) and Tothill (**B**) classifications of HGSOC cases included in the MITO16A case material. Numbers of patients at risk are reported below each Kaplan–Meier curve. In each panel, pie charts represent cases' distribution among the different molecular subtypes. **C** Expression of the CD8 gene in the MITO16A case material. **D** Distribution of CD8 gene among the molecular subtypes according to TCGA and Tothill classifications, considering all cases or HGSOC only. **E** Expression of the CD68 gene in the MITO16A case material. **F** Distribution of CD68 gene among the molecular subtypes according to TCGA and Tothill classifications, considering all cases or HGSOC only. For Tothill classifier: C1 = MES; C2 = IMM; C4 = DIFF; C5 = PRO.

Noteworthy, applying the two algorithms on the whole case material ($n = 197$ samples), which also includes tumor types other than HGSOC, we obtained essentially the same results (Fig. S3).

CD8 + T cells and M1-macrophages are the most enriched immune populations in the IMM/C2 subtype

To get insight into this particular behavior, starting from MITO16A-MaNGO OV-2 bulk transcriptome array data, we applied CIBERSORTx to infer the cell-type-specific GEP pattern of 22 immune-related cellular populations (Table S1). Then, for each immune-related CIBERSORTx population, we analyzed the relative distribution among the molecular subtypes obtained by applying both TCGA (Fig. S4) and Tothill (Fig. S5) classifiers and evaluated any significant variation (Table S2). T_cells_CD8, T_cells_CD4_memory_resting, Macrophages_M1, Dendritic_cells_resting, Dendritic_cells_activated, and Mast_cells_activated were the only populations showing significant variation among the molecular subtypes when applying both classifiers (Table S3).

Looking at the CIBERSORT populations with concordant significant modulation between the two classifiers, CD8 cells and Macrophages M1 resulted to be significantly enriched in the IMM/C2 subtype as compared to all other molecular subtypes, while CD4 cells and Mast_cells_activated were significantly enriched in the IMM/C2 subtype as compared to PRO/C5 subtype only (Figs. S4 and S5 and Table S4). In contrast, the PRO/C5 subtype turned out to have a significant decrease in dendritic cells (both resting and activated) compared to all other molecular subtypes, including IMM/C2 (Figs. S4 and S5).

We therefore focused on T_cells_CD8 and Macrophage_M1, the two immune populations we found specifically enriched in the immune-related molecular subtypes. The CD8 gene shows a comparable expression level in serous vs other histotypes (Fig. 1C). When we compared its expression among the molecular subtypes according to TCGA (Fig. 1D, left panels) and Tothill (Fig. 1D, right panels) classification, we observed that the CD8 gene has a significantly higher expression in the IMM/C2 subgroups, both considering all cases (Fig. 1D, upper panels) or HGSOC only (Fig. 1D, lower panels). Similarly, for the CD68 gene we found a comparable level of expression in serous vs other histotypes (Fig. 1E). When we compared its expression distribution among the molecular subtypes according to TCGA (Fig. 1F, left panels) and Tothill (Fig. 1F, right panels) classification, both considering all cases (Fig. 1F, upper panels) or HGSOC only (Fig. 1F, lower panels), we observed that CD68 expression was significantly higher in both immune-related and proliferative-related subgroups (Fig. 1F), the latter having the worse prognosis (Fig. 1A, B).

MIF and gene expression analyses correlate high CD8+ infiltration with worse prognosis

To get insights into any possible association of CD8 and Macrophage infiltrate with prognosis, we utilized multispectral imaging associated with MIF on the 292 samples that passed all the quality controls (see Fig. S1).

No differences in clinical and pathological variables were observed between patients included in biomarkers analyses ($n = 292$) and the whole MITO16A-MaNGO OV-2 trial population ($n = 398$) (Table 1).

All samples were stained for the expression of CD8 (to identify tumor-infiltrating T cells), CD68 (tumor-infiltrating monocyte/macrophages), cytokeratins (tumor cells), and nuclei. CD274 (PD-L1 positive cells) staining was also included, but has been reported elsewhere[28]. The five color-stained slides were then studied using a multispectral camera and computer-assisted

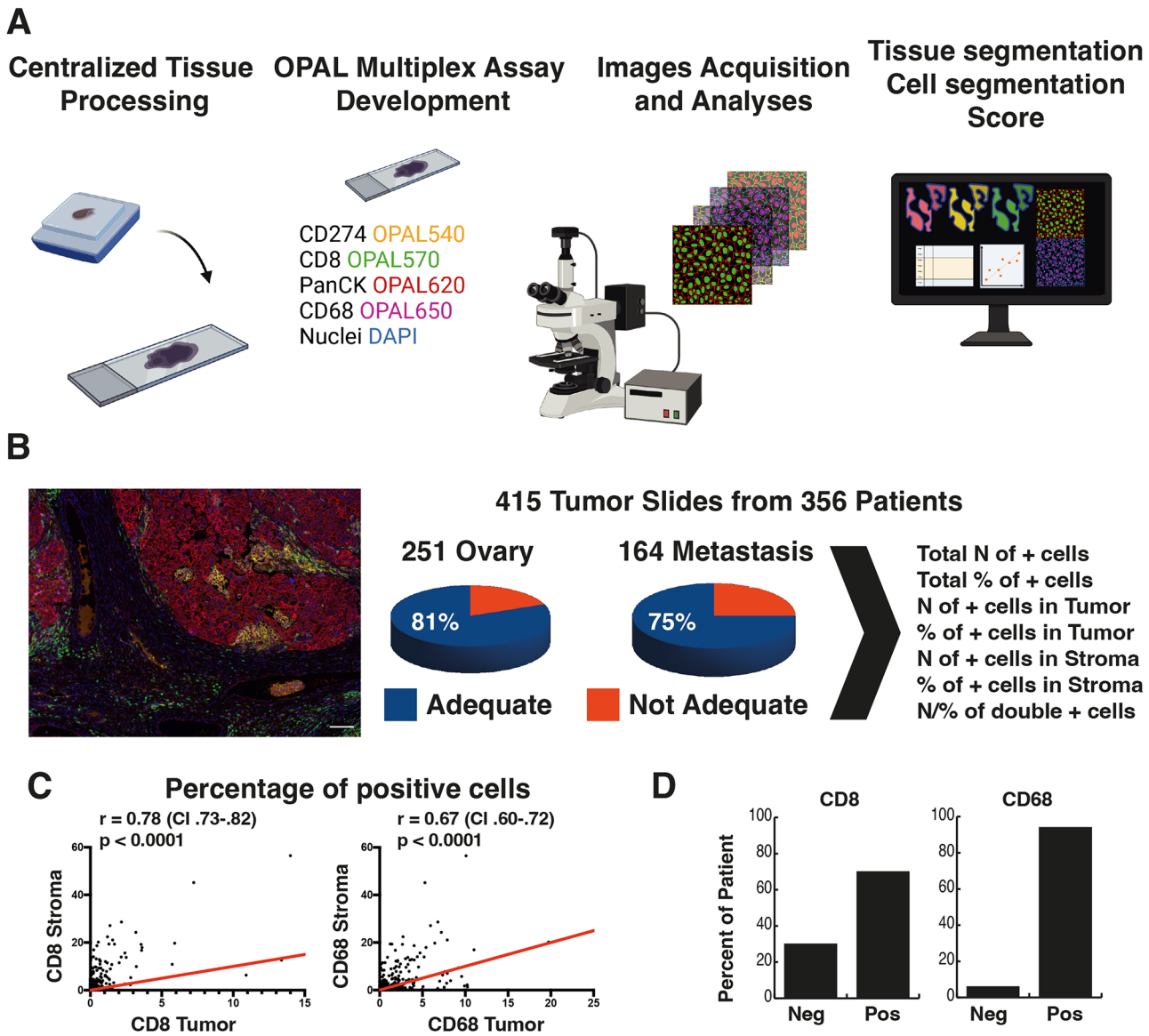

Fig. 2 | Multiplex staining evaluating tumor and stroma immune infiltration in samples from the MITO16A case material. A Scheme of the multiplex analyses using the OPAL Multiplex Assay coupled with multispectral image acquisition. Centralized tumor samples were processed, and single FFPE tissue slides were stained with the indicated antibodies for MIF. Stained sections were acquired with a Nikon microscope coupled with a multispectral camera, and acquired images were analyzed with the InForm software to define the number of immune cells infiltrating the tumors (PanCK-positive areas) and the surrounding stroma. Created with BioRender.com. **B** On the left, a typical image of immune cells infiltrating the tumor (color code as in **A**). Scale bar is 100 µm. On the right, pie charts report the number of analyzed slides that proved adequate or not for subsequent analyses after the multi-staining process. **C** Correlation between tumor and stroma infiltration in the same sample from $CD8^+$ (left graph) and $CD68^+$ (right graph) immune cells. **D** Graphs reporting the percentage of CD8 and CD68 immune-excluded (Neg) and immune-infiltrated (Pos) samples, as indicated.

analyses. This pipeline allowed us to determine the percentage and the location (intratumor vs stromal) of $CD8^+$ and $CD68^+$ immune cells (Figs. 2A, B and S6).

The analyses of $CD8^+$ and $CD68^+$ cells demonstrated a low to non-significant correlation between infiltrating $CD8^+$ and $CD68^+$ cells either in the stroma or in the tumor, among the different samples analyzed (Fig. S7). However, a moderate to high correlation was observed when the number of $CD8^+$ or $CD68^+$ cells infiltrating the tumor and the surrounding stroma of the same sample was analyzed (Fig. 2C). No association was found between CD8 and CD68 positivity and the common prognostic parameters, including age, FIGO Stage, tumor histology, and residual disease (Table S5). A variable proportion of immune-excluded patients was identified when CD8 and/or CD68 positivity was evaluated. In particular, 30% and 6% were completely negative for CD8 and CD68 cells, respectively (Fig. 2D).

In a small group of patients ($n = 32$) for whom primary and metastatic lesions taken at diagnosis were available, we observed a low correlation in the number of infiltrating CD8 and CD68 cells in the tumor or the stroma. A slight increase in the correlation values was observed when the total percentage of infiltrating CD68 and, especially, CD8 positive cells was considered (Fig. S8).

When analyzed as continuous variables in univariable or multivariable models, neither CD8 nor CD68 MIF score was associated with patients' prognosis for PFS and OS. However, low expression of $CD8^+$ cells in tumor and stroma tended to be associated with a better prognosis (Table S6). These results were quite unexpected due to the reported association between high T cell infiltration and longer patients' PFS in EOC[16–18]. We thus searched for both CD8 and CD68's best cutoff that minimizes the *p*-value of HR (details in "Methods"). Using these cutoff values in Kaplan–Meier curves, we

observed that high infiltration of $CD8^+$ but not $CD68^+$ cells in the tumor, stroma, or both was associated with a shorter PFS of enrolled patients (Fig. 3A, B). Importantly, when adjusted for over-fitting HRs estimates using the bootstrap-percentile method[29] total CD8 infiltration maintains its association with higher risk of shorter PFS (HR = 1.94; $p = 0.031$) (Table 2). The same was not true for the OS (Fig. S9).

We next tested the prognostic value of the same biomarkers in multivariable analyses adjusted for patients' clinical characteristics. Again, high $CD8^+$ infiltration was associated with shorter PFS (HR 1.94, $p = 0.014$) but not OS (Table S7). Tumor, stromal, or total infiltration of $CD68^+$ cells did not significantly predict patients' survival (Tables 2 and S7).

We were able to combine the MIF results with GE data on 171 patients to analyze the distribution of CD8 and CD68 staining along with the molecular subtypes. Paired analysis of CD8 and CD68 staining showed that patients with the worst prognosis, with a CD8 staining above the cutoff value, were also those having the highest CD68 staining score and were essentially in the PRO/C5 molecular subtype (Fig. 3C).

As a further exploratory analysis, based on the biological rationale that the categorization of patients with immune-desert 'cold' tumors vs high-infiltrating 'hot' tumors could better evidence the prognostic significance of immune infiltrate, we stratified patients according to the joint expression of CD8 and CD68 as assessed by MIF count. We identified the 'cold' subgroup corresponding to patients having MIF count < 1 for both markers and the 'positive' subgroup corresponding to those patients having both CD8 and CD68 MIF counts in the relative upper-quartile. We then explored the KM curves for PFS (upper panels) and OS (lower panels) in all case material (left) and in the HGSOC samples only (right) (Fig. S10). Being aware of the explorative nature of the analysis, we, however, observed a generally worse outcome for patients with a jointly high CD8 and CD68 staining as compared to those showing the cold phenotype, confirming the results obtained using the best cutoff method. Finally, we used quartile separation to verify if categorizing patients for the different amounts of infiltration could give us more insights into the prognostic value of tumor infiltration in EOC patients enrolled in this trial. Although the separation of cases into four groups diminished the statistical power of the analyses and rendered the differences not significant, we again observed that samples with low CD8 infiltration (1st quartile) were associated with a slightly longer PFS and OS, while samples with high infiltration (4th quartile) were associated with a slightly shorter PFS (Fig. S11A, C). No differences among groups were observed when CD68 infiltration was evaluated using quartile separation (Fig. S11B, D). Similar results were obtained when patients were stratified for median expression of CD8 or CD68 (Fig. S12). Again, although these are explorative analyses and should be taken with caution, we can confirm that high immune infiltrate did not associate with better prognosis for BEV-treated patients, as largely observed for EOC patients treated with BEV-free regimens.

Discussion

In this multidisciplinary effort, the MITO group applied spatial MIF coupled with the analyses of GE to explore the role of the immune infiltrate in the response to BEV-containing regimens in EOC patients, using samples from a Phase IV clinical trial specifically designed to identify prognostic biomarkers for EOC patients treated in first line with BEV-containing regimens. To our knowledge, this is the first large clinical trial in EOC (398 patients enrolled) in which spatial MIF was performed on all available samples, covering 89.4% of enrolled patients. We showed that spatial MIF, evaluating tumor and stromal immune infiltration, could provide additional information compared to the simple immunohistochemistry (IHC) studies and could be used to retrieve prognostic information.

The most interesting result we obtained is to clearly show that immune-infiltrating tumors are associated with shorter PFS of BEV-treated patients. This evidence, along with the notion that in EOC patients treated with BEV-free regimens the presence of immune infiltrating cells predicts a better survival[26], suggests that the evaluation of immune infiltrating $CD8^+$ cells in EOC could be used to select patients less likely to respond to BEV maintenance therapy. Interestingly, a recent study that applied our same approach to analyze data from the chemo-only arm of ICON-7 found that the immune-excluded/mesenchymal subtype had the worst PFS, reinforcing the concept that the immune infiltration has a completely different prognostic value for chemotherapy compared to BEV[30]. Similar observations were made by Liontos and collaborators, who reported that immune infiltration was associated with better PFS in patients treated with chemotherapy alone but not in those who also received BEV, in a small, monocentric retrospective study evaluating the prognostic value of immune infiltrate in EOC patients treated with neo-adjuvant chemotherapy[19].

When sample segmentation was used, the infiltration of CD8 cells in the stroma and in the tumor was also independently associated with a higher risk of relapse, although this association was statistically lost after adjusting for over-fitting HRs. Nevertheless, this information suggests that the presence/absence of $CD8^+$ cells in the tumor dictates the prognostic value more than their localization within the tumor mass. In this regard, we noticed a high proportion (30%) of $CD8^+$ cold tumors, a notion in line with the still unsuccessful attempts to use immunotherapy in EOC patients, and a low proportion of $CD68^+$ cold tumors (6%), in line with the reported higher macrophage polarization in immune-excluded and cold EOC[16].

We still do not know if BEV treatment could lead to an increase in tumor immune infiltration since we analyzed all samples at diagnosis. Yet, it has been suggested that the important synergy seen with PARPi and BEV treatment, specifically in patients with HGSOC tumors with homologous recombination deficiency (HRD) treated in the adjuvant setting in the PAOLA-1 study, could be due to the vascular reprogramming and T cell infiltration produced by VEGFA blockade[16,31]. This hypothesis merits a formal experimental demonstration.

Similarly, we do not know if the evaluation of immune infiltration at diagnosis could represent a predictive biomarker of response to BEV treatment. To answer this question and based on this positive MITO experience and the promising results obtained, we will evaluate the predictive role of the immune infiltrate using the samples already collected in the MITO16b/MANGO/-OV2/ENGOT-ov17 phase III randomized trial that compared BEV treatment to standard therapy at disease recurrence[32].

Finally, we would like to point out that accumulating evidence suggests that BRCA1/2 alterations and/or HRD are associated with high immune infiltrate in EOC[33,34]. Therefore, it is conceivable that high immune infiltrate could be more likely associated with better overall prognosis and sensitivity to PARPi. Nevertheless, we have to consider that the MITO16A trial and its prespecified analyses were designed in 2010, and the enrollment of the patients was performed from October 2012 to November 2014[22] when the evaluation of BRCA1/2 and HR status was not routinely performed in Italy. Thus, we cannot confidently rule out whether, in our case series, HRD is associated with a hot TME. Yet, using subpopulations of MITO16A, we proved that HRD, evaluated using different commercial and academic approaches, indeed associates with a better prognosis also in BEV-treated patients[35,36] in line with literature data.

This manuscript, however, suffers from some limitations that should be taken into consideration. First, the statistical design to calculate prognostic values of analyzed biomarkers needed the enrollment of 400 patients; although we met the expected patients' accrual, technical limitations reduced by one-third the number of samples analyzed by MIF and by half the number of patients analyzed by GE. Of note, 18% of processed samples could not be analyzed by MIF due to failure during the multiple staining procedures, suggesting that an optimization of staining processing is needed. We observed that the failures were more frequent in peritoneal metastatic localizations compared to primary ovarian cancer disease, and this notion could likely be useful in future studies, both in the choice and in the handling of samples to be analyzed. In any case, the large amount of collected and digitalized data could be useful in the future to develop artificial intelligence approaches that

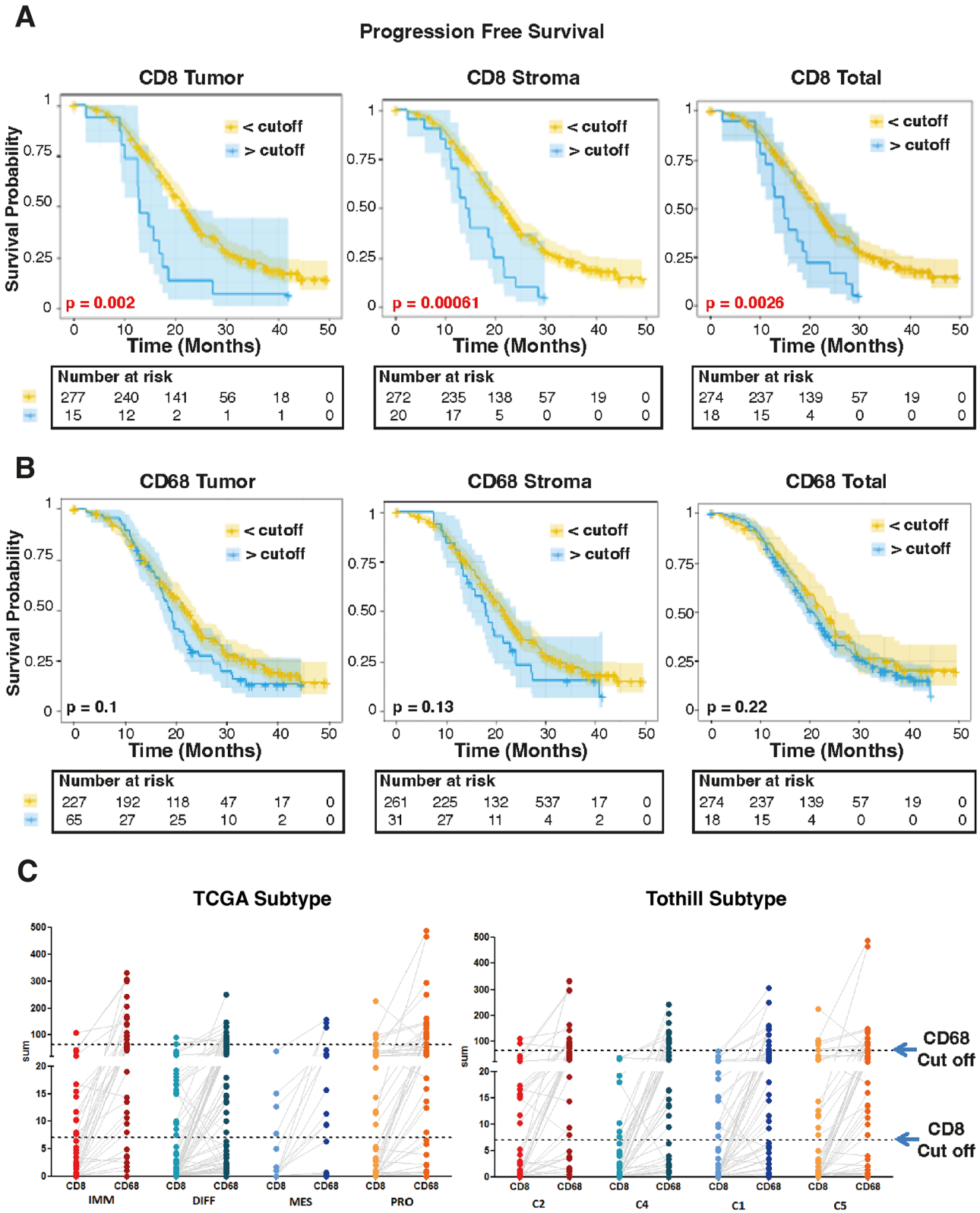

Fig. 3 | Prognostic values of CD8 and CD68 immune infiltration in analyzed cases. A Kaplan–Meier curves evaluating patients' PFS based on CD8 tumor, stromal, or total (sum of tumor and stromal) infiltration. Patients were stratified using the identified best cutoff values (see Table 2). **B** Kaplan–Meier curves evaluating patients' PFS based on CD68 tumor, stromal, or total (sum of tumor and stromal) infiltration using the identified best cutoff values (see Table 2). **C** Distribution of CD8 and CD68 combining MIF expression and GE data to stratify among the molecular subtypes according to TCGA (left panel) and Tothill (right panel).

Table 2 | Analysis of biomarkers best cutoff for PFS

PFS	Original			Adjusted for overfitting (bootstrap CI)		
	HR	(95% CI)	p	HR	(95% CI)	p
MODEL CD8						
Tumor > 40.3	**1.88**	**(1.06–3.35)**	**0.031**	1.64	(0.59–4.61)	0.344
Stroma > 26.5	**1.95**	**(1.18–3.23)**	**0.009**	1.77	(0.68–4.65)	0.245
MODEL CD68						
Tumor > 52.6	1.24	(0.89–1.72)	0.196	1.09	(0.46–2.6)	0.845
Stroma > 53.7	1.27	(0.83–1.95)	0.276	1.04	(0.46–2.36)	0.929
MODEL CD8						
Sum > 67.3	**2.11**	**(1.28–3.48)**	**0.003**	**1.94**	**(1.06–3.53)**	**0.031**
MODEL CD68						
Sum > 7.0	1.20	(0.9–1.61)	0.217	1.07	(0.48–2.38)	0.878

Best cutoff was calculated on MIF scores for CD8 or CD68 infiltration in tumor, stroma, or both (sum = tumor + stroma). In each model, patients were stratified according to the specific best cutoff value as specified in the Table.
HR hazard ratio, *CI* Confidence Interval, *p* *p*-value.
In bold, significant differences.

could better refine the significance of immune infiltration in EOC. Then, it is possible that the use of MIF could result in a different evaluation of immune cells when compared to classical IHC. However, recent evidence demonstrated a strong correlation between IHC staining and seven-color multiplex staining in ovarian cancer[37], and we also collected evidence that there is a strong correlation between IHC and MIF using CD274 expression in the MITO16A cohort[28].

The study also suffers from the lack of longitudinal data, since we could perform the analyses only on samples collected at diagnosis. This leaves unclear whether BEV treatment could lead to changes in immune infiltration over time, which is one of the biological rationales underlying the design of clinical trials evaluating the efficacy of combining BEV with immune-checkpoint inhibitors in EOC patients[38,39]. The results of these clinical trials were not as positive as expected, leaving it still uncertain whether immune-checkpoint inhibitors, alone or with antiangiogenic agents, merit being used to treat EOC patients and which are the most effective predictive biomarkers to select the patient population that could mostly benefit from this treatment[40–42]. Based on these considerations, it appears necessary to better dissect the biological mechanisms linking angiogenesis regulation and anti-tumor immunity using the most appropriate models and samples collected in prospective clinical trials with translational endpoints.

Finally, we did not investigate the functional status of immune cells in the TME, which may influence outcomes and the interpretation of immune infiltration data.

Based on these limitations, we cannot exclude that the observed association between immune infiltration and clinical outcome may represent a cohort-specific effect that is not generalizable beyond the studied population. Indeed, the absence of a chemotherapy-only comparator cohort precludes any substantiated conclusions regarding the predictive value of immune infiltration in the context of BEV-containing regimens.

We believe that these evidences merit further examination in future studies, possibly using samples from randomized clinical trials in which patients were treated with or without antiangiogenic agents. We propose that evaluating the presence and spatial distribution of immune infiltrate (especially $CD8^+$ cells) at the time of diagnosis may contribute, along with other analyses, to better personalizing the therapy of EOC patients. Specifically designed prospective trials in which immune infiltrate will be used to assist clinicians in their therapeutic decisions will be necessary to properly confirm this possibility.

Methods

Patients

MITO16A-MaNGO OV-2 is a phase IV multicenter single-arm registered trial (EudraCT number: 2012-003043-29, www.clinicaltrials.gov number: NCT01706120, Registered 24 September 2012) that aimed to explore the prognostic role of clinical and selected biological factors in EOC patients treated in first line with chemotherapy (Paclitaxel + Carboplatin x6) plus BEV (15 mg/kg) for 15 months[22]. The study was designed to have 80% power to identify a potential prognostic factor able to select a favorable subgroup with a 0.60 hazard ratio (HR), expressed in at least 20% of the population. With an alpha error of 0.01, 280 events (either PFS or OS) were required for the final analysis, and a sample size of 400 patients was planned[22]. The study was approved by the Ethics Committee (first approval by the Ethics Committee of the proponent institute INT Pascale Napoli, Prot. #383/12 of 19 July 2012) and all patients provided written informed consent. All procedures were carried out in accordance with the principles of the Declaration of Helsinki.

Three hundred and ninety-eight patients were enrolled in the study, and tissue sample collection was centralized at the INT G. Pascale of Naples, which supervised the quality controls and performed tissue processing, nucleic acid extraction then provided to final investigators with the biological material as necessary and described in refs. 23,43.

MIF analyses

Histological sections (5 µm) were made from the paraffin blocks. Whole tissue sections were used to evaluate the expression on the same slide of CD8 (T Lymphocytes), CD68 (Macrophages), CD274 (PD-L1 Positive cells), and Cytokeratins (Pan-CK, tumor cells). DAPI was used to stain cell nuclei. Of the 398 patients enrolled in the MITO16A-MaNGO OV-2 phase 4 trial who agreed to donate their samples for translational studies, 42 were excluded for technical reasons. Samples from 356 patients were analyzed by MIF, and 64 patients were excluded at this stage for technical reasons (see Consort Fig. S1).

Before proceeding with MIF, 5 µm-thick sections were deparaffinated, rehydrated, and subjected to epitope retrieval through microwave treatment. To perform MIF, slides were stained with Opal 7 Immunology Discovery Kit (OP7DS1001KT, PerkinElmer) according to the manufacturer's instructions. Slides were subjected to MIF by consecutive staining in the following order: CD8, CD68, PD-L1, and pan cytokeratins (PanCK). Anti-CD8 and CD68 were provided in the OP7DS1001KT (PerkinElmer). Anti-PD-L1 (E1L3N®) XP® Rabbit mAb was from Cell Signaling (Cell Signaling Technology Cat# 13684). Anti-PanCK mAb was from Roche (clone AE1/AE3/PCK26 Ventana).

Briefly, sections were rinsed, blocked with antibody diluent (ARD1001EA, PerkinElmer), incubated with the appropriate primary and secondary antibodies, and tyramide signal amplification (TSA) visualization was carried out with the marker assigned OPAL. After each staining round, antibody labeling was followed by an epitope retrieval step (using an appropriate buffer, according to primary antibody requirements) and a blocking step. Slides were counterstained with Spectral DAPI reagent (PerkinElmer). MIF images were acquired using the MANTRA System (Mantra 1.0.2, PerkinElmer). Single-plex stained slides, one for each OPAL fluorochrome used in this study, and DAPI, were applied to build the spectral library. Multispectral fluorescent images were analyzed using the inForm software (in Form 2.4.1, PerkinElmer). First, MIF images were unmixed by applying the spectral library, and the autofluorescence signal was removed. Then, images were analyzed with inForm software by means of tissue segmentation, cell segmentation, and positive score. At least three fields at 20× magnification were acquired for each sample.

GEP and data analysis

Of the 358 centralized FFPE blocks available for IHC analyses, 290 had sufficient and adequate material also for nucleic acids extraction (after pathological revision, cores were selected to represent at least a percentage > 70% of tumor cells and no significant signs of necrosis)[43].

RNA Quality checking was performed with the GeneChip WT Pico kit (Affymetrix, Thermo Fisher Scientific) following the guidelines for FFPE material. RNA extracted from 272 of these samples was then used for GEP. Probes were hybridized on human Clariom D chips (Affymetrix) and scanned with an Affymetrix Gene Chip Scanner 3000 7 G. Primary data acquisition and analysis of the generated CEL files were performed as described in ref. 44. The final data matrix includes about 28,000 unique genes.

We decided to rely on data derived from tumors collected at the primary site. From the 272 patients with RNA of adequate quality for GE, 67 were excluded since the FFPE blocks were derived from metastatic localizations (63 patients) or from undefined localizations (4 patients). Data from 8 more patients were excluded due to hybridization problems. GE data were therefore available for 197 patients; of these, 171 had also MIF data available.

Further analyses were performed using R [(R Foundation for Statistical Computing, Vienna, Austria) http://www.R-project.org], version 4.1.2, to challenge, in our dataset, the molecular profiles identified by Tothill[24,45] and TCGA[25]. For molecular subtypes' classification, samples were assigned to molecular subtypes according to different classification schemes using the *consensusOV* package (R-Bioconductor)[27]. The package achieves four major subtype classifiers for HGSOC as described by refs. 25,26,45,46. The TCGA-related classification (Verhaak) and the Helland (Tothill) classification were considered for downstream analysis. Immunoreactive (IMM), differentiated (DIFF), proliferative (PRO and mesenchymal (MES) were the subtypes identified according to the TCGA classifier, while C1, C2, C4, and C5 those classified according to Tothill, corresponding respectively to the MES, IMM, DIFF, PRO subtypes.

To infer the relative proportion of 22 types of infiltrating immune cells, normalized GE data were uploaded to the CIBERSORT web portal (http://cibersort.stanford.edu/) and the CIBERSORT/Tx algorithm was applied in the absolute mode. Association between immune cell type abundance and each molecular subtype was assessed by the Wilcoxon test, and *p*-values were adjusted using the Benjamini–Hochberg false discovery rate (FDR) procedure.

Statistical analyses

Statistical analyses have been performed as thoroughly described in the ref. 23. Briefly, for all biomarkers analyzed, a histogram was used to describe the distribution. A scatterplot and a modified version of the Kendall test for zero-inflated values were used to test the correlation between biomarkers[47].

The associations between each biomarker and the clinical prognostic factors were investigated using the Wilcoxon rank test for zero-inflated data (ZIW) for dichotomous variables and the Kruskal–Wallis zero-inflated (ZIKW) for categorical variables, using a permutation test. The prognostic effect of each biomarker was evaluated using PFS and OS as endpoints.

Kaplan–Meier curves were drawn for PFS and OS and compared with a two-sided log-rank test.

To test the prognostic role of each biomarker on both PFS and OS, univariable and multivariable Cox proportional models were performed.

In univariable analysis, each biomarker was tested as a categorical variable using a biologically relevant cutoff or after searching for the best cutoff value that minimizes the *p*-value of HR. The best cutoff was selected by choosing the value that minimized the *p*-value of HR on PFS and then applied to the OS.

For each biomarker, a multivariable analysis was performed using as covariates: age (as category <65 vs ≥65), ECOG performance status (PS) (0 vs 1–2), residual disease (none; ≤1 cm; >1 cm; not operated), FIGO stage (III vs IV) and Tumor histology (high-grade serous vs other). A shrinkage procedure with 95% CI was calculated with the bootstrap-percentile method[29] to adjust for over-fitting HRs estimates of the best cutoff categories. Data were analyzed using R software version 3.6.0 (R Foundation for Statistical Computing, Vienna, Austria), Prism 8.2.0, (GraphPad Software Inc.), and STATA/MP 14.1 (StataCorp LP, College Station, TX).

Data availability

Microarray data for human samples were compliant with MIAME (Minimum Information About a Microarray Experiment) guidelines and were deposited into the Gene Expression Omnibus (GEO) database of NCBI (National Center for Biotechnology Information) (http://www.ncbi.nlm.nih.gov/geo/), with accession numbers GSE208103.

Code availability

Not applicable.

Received: 5 June 2025; Accepted: 1 October 2025;
Published online: 17 November 2025

References

1. González-Martín, A. et al. Newly diagnosed and relapsed epithelial ovarian cancer: ESMO Clinical Practice Guideline for diagnosis, treatment and follow-up. *Ann. Oncol.* **34**, 833–848 (2023).
2. Ledermann, J. A. et al. ESGO-ESMO-ESP consensus conference recommendations on ovarian cancer: pathology and molecular biology and early, advanced and recurrent disease. *Ann. Oncol.* **35**, 248–266 (2024).
3. Presta, L. G. et al. Humanization of an anti-vascular endothelial growth factor monoclonal antibody for the therapy of solid tumors and other disorders. *Cancer Res.* **57**, 4593–4599 (1997).
4. Burger, R. A. et al. Incorporation of bevacizumab in the primary treatment of ovarian cancer. *N. Engl. J. Med.* **365**, 2473–2483 (2011).
5. Oza, A. M. et al. Standard chemotherapy with or without bevacizumab for women with newly diagnosed ovarian cancer (ICON7): overall survival results of a phase 3 randomised trial. *Lancet Oncol.* **16**, 928–936 (2015).
6. Perren, T. J. et al. A phase 3 trial of bevacizumab in ovarian cancer. *N. Engl. J. Med.* **365**, 2484–2496 (2011).
7. Karam, A. et al. Fifth ovarian cancer consensus conference of the Gynecologic Cancer Intergroup: first-line interventions. *Ann. Oncol.* **28**, 711–717 (2017).
8. Tewari, K. S. et al. Final overall survival of a randomized trial of bevacizumab for primary treatment of ovarian cancer. *JCO* **37**, 2317–2328 (2019).
9. Hu, B. et al. Systemic immune-inflammation index predicts prognosis of patients after curative resection for hepatocellular carcinoma. *Clin. Cancer Res.* **20**, 6212–6222 (2014).
10. Passardi, A. et al. Inflammatory indexes as predictors of prognosis and bevacizumab efficacy in patients with metastatic colorectal cancer. *Oncotarget* **7**, 33210–33219 (2016).
11. Huang, Q.-T. et al. Prognostic significance of neutrophil-to-lymphocyte ratio in ovarian cancer: a systematic review and meta-analysis of observational studies. *Cell Physiol. Biochem.* **41**, 2411–2418 (2017).
12. Farolfi, A. et al. Inflammatory indexes as prognostic and predictive factors in ovarian cancer treated with chemotherapy alone or together with bevacizumab. A multicenter, retrospective analysis by the MITO group (MITO 24). *Target Oncol.* **13**, 469–479 (2018).
13. Farolfi, A. et al. Inflammatory indexes as predictive factors for platinum sensitivity and as prognostic factors in recurrent epithelial ovarian cancer patients: a MITO24 retrospective study. *Sci. Rep.* **10**, 18190 (2020).
14. Galon, J. & Bruni, D. Approaches to treat immune hot, altered and cold tumours with combination immunotherapies. *Nat. Rev. Drug Discov.* **18**, 197–218 (2019).
15. Schoutrop, E. et al. Molecular, cellular and systemic aspects of epithelial ovarian cancer and its tumor microenvironment. *Semin Cancer Biol.* **86**, 207–223 (2022).
16. Kandalaft, L. E., Dangaj Laniti, D. & Coukos, G. Immunobiology of high-grade serous ovarian cancer: lessons for clinical translation. *Nat. Rev. Cancer* **22**, 640–656 (2022).

17. Santoiemma, P. P. & Powell, D. J. Tumor infiltrating lymphocytes in ovarian cancer. *Cancer Biol. Ther.* **16**, 807–820 (2015).
18. Hwang, W.-T., Adams, S. F., Tahirovic, E., Hagemann, I. S. & Coukos, G. Prognostic significance of tumor-infiltrating T cells in ovarian cancer: a meta-analysis. *Gynecol. Oncol.* **124**, 192–198 (2012).
19. Liontos, M. et al. Lymphocytic infiltration and chemotherapy response score as prognostic markers in ovarian cancer patients treated with neoadjuvant chemotherapy. *Gynecol. Oncol.* **157**, 599–605 (2020).
20. Kommoss, S. et al. Bevacizumab may differentially improve ovarian cancer outcome in patients with proliferative and mesenchymal molecular subtypes. *Clin. Cancer Res.* **23**, 3794–3801 (2017).
21. Gourley, C. et al. Molecular subgroup of high-grade serous ovarian cancer (HGSOC) as a predictor of outcome following bevacizumab. *J. Clin. Oncol.* https://doi.org/10.1200/jco.2014.32.15_suppl.5502 (2014).
22. Daniele, G. et al. Bevacizumab, carboplatin, and paclitaxel in the first line treatment of advanced ovarian cancer patients: the phase IV MITO-16A/MaNGO-OV2A study. *Int. J. Gynecol. Cancer* **31**, 875–882 (2021).
23. Califano, D. et al. Evaluation of angiogenesis-related genes as prognostic biomarkers of bevacizumab treated ovarian cancer patients: results from the phase IV MITO16A/ManGO OV-2 translational study. *Cancers* **13**, 5152 (2021).
24. Tothill, R. W. et al. Novel molecular subtypes of serous and endometrioid ovarian cancer linked to clinical outcome. *Clin. Cancer Res.* **14**, 5198–5208 (2008).
25. Verhaak, R. G. W. et al. Prognostically relevant gene signatures of high-grade serous ovarian carcinoma. *J. Clin. Invest.* **123**, 517–525 (2013).
26. Konecny, G. E. et al. Prognostic and therapeutic relevance of molecular subtypes in high-grade serous ovarian cancer. *J. Natl. Cancer Inst.* **106**, dju249 (2014).
27. Chen, G. M. et al. Consensus on molecular subtypes of high-grade serous ovarian carcinoma. *Clin. Cancer Res.* **24**, 5037–5047 (2018).
28. Basso-Valentina, F. et al. Programmed death-ligand 1 expression and prognostic significance in bevacizumab treated ovarian cancer patients: results from the phase IV MITO16A/MaNGO OV-2 translational study. *Clin. Transl. Med.* **15**, e70373 (2025).
29. Holländer, N., Sauerbrei, W. & Schumacher, M. Confidence intervals for the effect of a prognostic factor after selection of an 'optimal' cutpoint. *Stat. Med.* **23**, 1701–1713 (2004).
30. Desbois, M. et al. Integrated digital pathology and transcriptome analysis identifies molecular mediators of T-cell exclusion in ovarian cancer. *Nat. Commun.* **11**, 5583 (2020).
31. Ray-Coquard, I. et al. Olaparib plus bevacizumab as first-line maintenance in ovarian cancer. *N. Engl. J. Med.* **381**, 2416–2428 (2019).
32. Pignata, S. et al. Carboplatin-based doublet plus bevacizumab beyond progression versus carboplatin-based doublet alone in patients with platinum-sensitive ovarian cancer: a randomised, phase 3 trial. *Lancet Oncol.* **22**, 267–276 (2021).
33. Vázquez-García, I. et al. Ovarian cancer mutational processes drive site-specific immune evasion. *Nature* **612**, 778–786 (2022).
34. van Wagensveld, L. et al. Homologous recombination deficiency and cyclin E1 amplification are correlated with immune cell infiltration and survival in high-grade serous ovarian cancer. *Cancers* **14**, 5965 (2022).
35. Capoluongo, E. D. et al. Alternative academic approaches for testing homologous recombination deficiency in ovarian cancer in the MITO16A/MaNGO-OV2 trial. *ESMO Open* **7**, 100585 (2022).
36. Roma, C. et al. Harmonization of homologous recombination deficiency testing in ovarian cancer: Results from the MITO16A/MaNGO-OV2 trial. *Eur. J. Cancer* **206**, 114127 (2024).
37. Lara, O. D. et al. Tumor core biopsies adequately represent immune microenvironment of high-grade serous carcinoma. *Sci. Rep.* **9**, 17589 (2019).
38. Shrimali, R. K. et al. Antiangiogenic agents can increase lymphocyte infiltration into tumor and enhance the effectiveness of adoptive immunotherapy of cancer. *Cancer Res.* **70**, 6171–6180 (2010).
39. Motz, G. T. et al. Tumor endothelium FasL establishes a selective immune barrier promoting tolerance in tumors. *Nat. Med.* **20**, 607–615 (2014).
40. Moore, K. N. et al. Atezolizumab, bevacizumab, and chemotherapy for newly diagnosed stage III or IV ovarian cancer: placebo-controlled randomized phase III trial (IMagyn050/GOG 3015/ENGOT-OV39). *J. Clin. Oncol.* **39**, 1842–1855 (2021).
41. Freyer, G. et al. Bevacizumab, olaparib, and durvalumab in patients with relapsed ovarian cancer: a phase II clinical trial from the GINECO group. *Nat. Commun.* **15**, 1985 (2024).
42. Banerjee, S. et al. Bevacizumab, atezolizumab and acetylsalicylic acid in recurrent, platinum-resistant ovarian cancer: the EORTC 1508-GCG phase II study. *Clin. Cancer Res.* https://doi.org/10.1158/1078-0432.CCR-24-3368 (2025).
43. Califano, D. et al. Ovarian cancer translational activity of the Multicenter Italian Trial in Ovarian Cancer (MITO) group: lessons learned in 10 years of experience. *Cells*. https://doi.org/10.3390/cells9040903 (2020).
44. Forlani, L. et al. Biological and clinical impact of membrane EGFR expression in a subgroup of OC patients from the phase IV ovarian cancer MITO-16A/MANGO-OV2A trial. *J. Exp. Clin. Cancer Res.* **42**, 83 (2023).
45. Helland, Å et al. Deregulation of MYCN, LIN28B and LET7 in a molecular subtype of aggressive high-grade serous ovarian cancers. *PLoS One* **6**, e18064 (2011).
46. Bentink, S. et al. Angiogenic mRNA and microRNA gene expression signature predicts a novel subtype of serous ovarian cancer. *PLoS One* **7**, e30269 (2012).
47. Pimentel, R. S., Niewiadomska-Bugaj, M. & Wang, J.-C. Association of zero-inflated continuous variables. *Stat. Probab. Lett.* **96**, 61–67 (2015).

Acknowledgements

We are grateful to the patients who consented to donating their tumor samples and to all the members of the MITO group for their support. This work was supported by grants from: the CRO Aviano Ricerca Corrente core grant (linea 1) of Ministero della Salute (G. Baldassarre); the Associazione Italiana Ricerca sul Cancro (AIRC) (IG 26253) (G. Baldassarre); the Alleanza Contro il Cancro (ACC) (RCR-2022-23682287) (G. Baldassarre); the Ministero della Salute (PNRR-MAD-2022-12375663) (G. Baldassarre); the Ministero Università e Ricerca (MIUR) (ARS01_00568) (G. Baldassarre); the Ministero della Salute (CO-2018-12367051) (S. Pignata); the Associazione Italiana Ricerca sul Cancro (AIRC) (IG25932) (S. Pignata); the IRCCS G. Pascale Napoli Ricerca Corrente L3/13 of Ministero della Salute (S. Pignata); the Associazione Italiana Ricerca sul Cancro (AIRC) (IG26066) (M. Bagnoli); and the Associazione Italiana Ricerca sul Cancro (AIRC) (Italy Post-Doc Fellowship 29639 and 31335) (F. Basso-Valentina). Fig. 2A was created with BioRender.

Author contributions

E.P.: data curation and investigation. V.C.: data curation and investigation. M.B.: data curation, formal analysis, investigation, visualization, writing—original draft, and writing—review and editing. P.C.: data curation, formal analysis, and writing—review and editing. A.S.: investigation. LA: data curation and formal analysis. D.L.: resources. G.T.: resources. S.C.C.: resources. A.F.: resources. G.S.: investigation. F.B.-V.: investigation, visualization, and writing—review and editing. D.C.: data curation, investigation, and writing—review and editing. L.D.C.: investigation. T.D.L.: investigation. M.S.N.: investigation. M.A.: investigation and writing—review

and editing. D.R.: investigation. P.S.: investigation. S.I.: investigation, methodology, supervision, validation, visualization, writing—original draft, and writing—review and editing. D.M.: supervision, validation, writing—original draft, and writing—review and editing. F.P.: supervision. S.P.: conceptualization, funding acquisition, project administration, resources, software, supervision, writing—original draft, and writing—review and editing. G.B.: conceptualization, funding acquisition, project administration, software, supervision, validation, visualization, writing—original draft, and writing—review and editing. All authors read and approved the manuscript.

Competing interests

The authors declare no competing interests.

Additional information

Supplementary information The online version contains supplementary material available at https://doi.org/10.1038/s41698-025-01146-7.

Correspondence and requests for materials should be addressed to Gustavo Baldassarre.

[1]Molecular Oncology Unit, Centro di Riferimento Oncologico di Aviano (CRO), IRCCS, National Cancer Institute, Aviano, Italy. [2]Pathology Unit, IRCCS CRO Aviano-National Cancer Institute, Aviano, Italy. [3]Department of Medical, Surgical and Health Sciences, University of Trieste, Trieste, Italy. [4]Fondazione IRCCS Istituto Nazionale dei Tumori, Milano, Italy. [5]Department of Mental Health and Public Medicine, Section of Statistics, Università degli Studi della Campania Luigi Vanvitelli, Milano, Italy. [6]Microenvironment Molecular Targets Unit, Istituto Nazionale Tumori IRCCS—Fondazione G. Pascale, Napoli, Italy. [7]Clinical Trials Unit, Istituto Nazionale Tumori IRCCS—Fondazione G. Pascale, Napoli, Italy. [8]Department of Woman and Child Health, Fondazione Policlinico Universitario A. Gemelli IRCCS, Rome, Italy. [9]Oncology 2 Unit, Veneto Institute of Oncology IOV-IRCCS, Padova, Italy. [10]Urogynaecological Medical Oncology, Istituto Nazionale Tumori IRCCS—Fondazione G. Pascale, Napoli, Italy. [11]Gynecology and Obstetrics Unit, Umberto I Hospital of Turin, Department of Surgical Sciences, University of Turin, Turin, Italy. [12]Pathology Unit, Istituto Nazionale Tumori IRCCS, Fondazione G. Pascale, Napoli, Italy. [13]Clinic of Obstetrics and Gynecology, 'S. Maria della Misericordia' University Hospital, Azienda sanitaria universitaria Friuli Centrale, Udine, Italy. [14]Department of Surgery, Oncology, Gastroenterology, University of Padova, Padua, Italy. [15]Basic and Translational Oncology Unit, Veneto Institute of Oncology IOV-IRCCS, Padova, Italy. [16]Present address: Clinical Pathology Unit, ASFO "Santa Maria degli Angeli" Hospital of Pordenone, Pordenone, Italy. [17]Present address: Faculty of Medicine and Surgery, Humanitas University, Milan, Italy, and Operative Unit of Gynecologic Oncology, Humanitas San Pio X, Milan, Italy. [18]These authors contributed equally: Eliana Pivetta, Vincenzo Canzonieri, Marina Bagnoli. [19]These authors jointly supervised this work: Sandro Pignata, Gustavo Baldassarre. ✉e-mail: gbaldassarre@cro.it